Natural Rubber Composites for Paper Coating Applications †

Pieter Samyn [1], Frank Driessen [2] and Dirk Stanssens [2],*

[1] Institute for Materials Research (IMO-IMOMEC), Applied and Analytical Chemistry, University of Hasselt, 3500 Hasselt, Belgium; Pieter.Samyn@uhasselt.be

[2] Topchim N.V. (a Solenis International LCC Company), 2160 Wommelgem, Belgium; FDriessen@solenis.com

* Correspondence: DStanssens@solenis.com; Tel.: +32-11-26-84-95

† Presented at the 2nd Coatings and Interfaces Web Conference, 15–31 May 2020; Available online: https://ciwc2020.sciforum.net/.

Abstract: Natural rubbers are characterized by extremely high molecular weight that might be beneficial in the formation of a protective barrier layer on paper substrates, providing good cohesive properties but limited adhesion to the substrate. In parallel, the low glass transition temperature of natural rubber might give the opportunity for good sealability, in contrast with severe problems of tack. Therefore, natural rubbers can be good candidates to serve as an alternative ecological binder in paper coatings for water and grease barrier resistance. In order to tune the surface properties of the paper coating, the effect of different fillers in natural rubber coatings are evaluated on rheological, thermo–mechanical and surface properties. The fillers are selected according to common practice for the paper industry, including talc, kaolinite clay and a type of organic nanoparticle, which are all added in the range of 5 to 20 wt.-%. Depending on the selected natural rubber, the dispersibility range (i.e., dispersive and distributive mixing) of the fillers in the latex phase highly varies and filler/matrix interactions are the strongest for nanoparticle fillers. An optimum selection of viscosity range allows us to obtain homogeneous mixtures without the need of surface modification of the additives. After bar-coating natural rubber latex composites on paper substrates, the drying properties of the composite coatings are followed by spectroscopy, illustrating the influences of selected additives on the vulcanization process. In particular, the latter most efficiently improves in the presence of nanoparticle fillers and highly increases the coating hydrophobicity in parallel, reducing the adhesive tack surface properties, as predicted from calculated work of adhesion.

Keywords: paper; biopolymer; fillers; rheology; contact angle; adhesion

1. Introduction

The demand for bio-based solutions in paper coating technology is urgent to replace oil-based polymers building protective coatings with high hydrophobicity. However, many biomaterials, such as cellulose, starch, carbohydrates, proteins, and glycerol, have hydrophilic properties and provide a solution for oil-barrier properties, but the range of hydrophobic biopolymers is more restricted. As an alternative, natural rubbers have intrinsic hydrophobic properties and are naturally dispersed in an aqueous latex phase, providing molecular structures with extremely high molecular weight. However, the material is often difficult to process into coating layers and its stability relies on the natural stabilization of the polyisoprene particles in the latex phase. On the other hand, the low glass transition temperatures of natural rubbers are favorable for the formation of film properties with rubbery characteristics at room temperature. The natural rubbers were applied as film former in

pharmaceutical coatings [1]: while providing excellent physical properties, such as high elasticity, high tensile strength and ease of film-forming, the films are soft and sticky [2]. The use of natural rubber as paper coatings is less developed, although the application on paperboard provides low water affinity and low absorption rates of the coated surfaces [3]. Although it has good potential to replace unrecyclable wax coating material on packaging papers, the blocking (sticking) tendency needs to be decreased with the content increase fillers—e.g., adding modified lignin can efficiently reduce the sticking problem of the coating [3]. In combination with cellulose fabrics, the natural rubber coatings were applied in a calendaring machine with good adhesion to the substrate, which is presumably due to the good mechanical and chemical compatibility of natural rubber and lignocellulose fibers [4].

In order to tune the composition and properties of the natural rubber coatings, additives are required to provide the requested surface properties, although compatibility with rheological properties and the molecular profile of the natural rubber should be investigated. In this work, typical coating fillers used in paper technology, including kaolinite, talc and organic styrene–maleimide nanoparticles, are used in combination with a natural rubber latex binder in order to investigate the effects on the processing and surface properties of the coating.

2. Materials and Methods

2.1. Materials

Vytex Natural Rubber Latex (Vystar, Worcester, MA, USA) was used as a commercially available "ultra-low protein" natural rubber latex with an intrinsic solid content of 60% (*w/w*) and pH = 10.4. Three different types of fillers were used, including kaolinite (KAO) powder with particle diameter < 2 μm and aspect ratio 20:1 (Imerys, Paris, France), talc powder, and styrene–maleimide (SMI) nanoparticles that were in-house synthesized according to a previous protocol [5]. The latex was used in non-diluted conditions for mixing with different filler types in concentrations of 5, 10, 20% (wt./wt.), using a three-blade propeller mixer under constant medium shear for about 1 h.

The mixed latex suspensions were applied as a paper coating on a laboratory scale K303 Multi-coater (RK Print Coat Instruments Ltd., Litlington, Royston, Hertfordshire, UK), using a black metering bar number 4 (close wound wire diameter 0.51 mm) resulting in a wet film thickness of about 40 μm. The coatings were dried for 2 min in a hot-air oven and further dried for one week under environmental lab conditions (23 °C; 50% RH). A reference paper grade was used for deposition of the films, including bleached Kraft pulp and internal sizing (350 μm thickness). In parallel, free standing rubber films of the same composition were cast on a PTFE foil for following adhesion measurements (the free films were more flexible and used as counterpart for an adhesive loop test).

2.2. Characterization

Rheological measurements on mixed latex suspensions were performed on Ares G2 equipment (TA Instruments) with a cylindrical bob-cup geometry operating at a gap distance of 2.10 mm. A suspension volume of 20.1 mL was added into the cup and first kept at rest for about 30 min before testing to relieve internal stresses. A continuous rotational shear test was performed under controlled shear rate between 0 and 1000 s^{-1} at a controlled temperature of 25 °C, while applying three subsequent sequences of ramp up (15 min)–rest at 1000 s^{-1} (5 min)–ramp down (15 min)–rest at 0 cm^{-1} (5 min)–ramp up (15 min), monitoring viscosity changes by eventual effects of hysteresis and/or internal history.

The differential scanning calorimetry (DSC) measurements were done on a Q200 equipment (TA Instruments) on a sample mass of 8.5 mg in a heating range from −90 to 180 °C at 20 °C/min under continuous nitrogen flow. The results for T_g (glass transition temperature) and Δc_p (heat capacity) are taken from the second heating step and averaged from two samples.

Attenuated total reflection Fourier transform infrared spectroscopy (ATR-FTIR) was done on separate natural rubber films (no paper coating) in order to focus on the effect of the fillers on the coating structure, without interfering spectral bands of the base paper. The measurements were done

on a Vertex 70 station (Bruker, Karlsruhe, Germany) with a diamond crystal (PIKE), collecting the spectra in a spectral range of 600–4000 cm^{-1} with a resolution of 4 cm^{-1}. A DTGS detector was installed to summarize 32 scans for 1 spectrum.

The scanning electron microscopy (SEM) was done on a Tabletop TM3000 microscope (Hitachi, Krefeld, Germany) under an acceleration voltage of 15 kV and backscattered secondary electron compositional mode. The magnification of 4000× was operated under a working distance of 8400 μm.

The other paper surface properties were determined by static contact angle measurements of deionized water and diiodomethane, applying a sessile drop method with drop volume of 2 μmL (water) and 0.8 μl (CH$_2$I$_2$), respectively. The adhesive properties of the coated paper surfaces were evaluated by an adhesive loop test on rubber films in contact with the coated paper of the same rubber composition, using a universal tensile tester (Schimadzu, Kyoto, Japan). A representative geometry of a film loop with width of 1 cm and length of 5 cm was clamped in between the upper dies and brought to a distance of 1 cm above the coated paper substrate that was horizontally fixed in the lower dies. The tack is characterized as the maximum force upon withdrawal of the rubber film from the coated paper surface, where experimental values of adhesive force are comparable due to the constant geometries.

3. Results

3.1. Rheological Properties

The rheological properties of the coating suspensions are presented as the variation of shear viscosity as a function of shear rates over three subsequent cycles, as given in Figure 1. The curves are recorded for suspensions with different fillers relative to the native natural rubber latex with solid content 60% (note: the viscosity scale of the materials is different for most detailed representations of the values). All filler types increased the viscosity of the original rubber latex to a different extent; however, all of them showed a shear-thinning effect with decreasing viscosity as a function of shear rate. The shear thinning behavior is enhanced in the presence of the fillers in most cases. The highest viscosities are observed for kaolinite fillers with an almost linear decrease in viscosity with shear rate at the highest concentrations, while the hysteresis of the kaolinite fillers is relatively low. This indicates the presence of strong mixing interactions between the kaolinite fillers and strong interactions with the natural rubber latex. The viscosity increase for SMI nanoparticles is significant with a more pronounced shear thinning effect, as the orientation of the nanoparticles under shear may additionally influence the structure of the suspension. The viscosity effects of nanoparticles are different from the microsize kaolinite, as an increase in nanoparticle concentration involves a decrease in viscosity. Therefore, it can be concluded from a viscosity-reducing effect of the nanoparticles that shear-induced mechanisms are influencing the nanoparticle mobility in the suspension and eventually lead to the orientation effects. The effects of reorganization of nanofillers in the rubber latex is also indicated by the relatively high hysteresis observed between the first and second ramp-up sequences for all concentrations, which was not observed for kaolinite fillers. Indeed, the nanoscale particles may have stronger influence on the latex flow properties compared to microscale particles. The latter are minimized in the case of talcum fillers, where very little alterations in viscosity and shear thinning effects are observed compared to the native rubber latex. However, the hysteresis effects for talc are also more pronounced than for kaolinite as it may be expected that the talc has a platelet structure that can be affected more by orientation effects under flow, while the kaolinite particles have a rather symmetrical shape. As it is observed that the viscosity for intermediate talc concentrations of 10 wt.-% decreases and the viscosity for the high talc concentrations of 20 wt.-% increases, the possible benefits of the orientation of the platelet structures are optimized at intermediate concentrations and hindered at the highest concentrations, where the highest concentrations might eventually lead to platelet–platelet interactions rather than platelet–latex interactions. The chemical interactions between the fillers and the natural rubber latex were not further studied at this stage, but besides particle shape, they can be attributed to specific surface interactions owing to the functional groups at the surface of the fillers, size distribution of the fillers and/or variations in zeta potential. While the present aim is to provide a view on the influence of the rheological

properties on the coating formation, the latter interactions are the subject of more fundamental study in future.
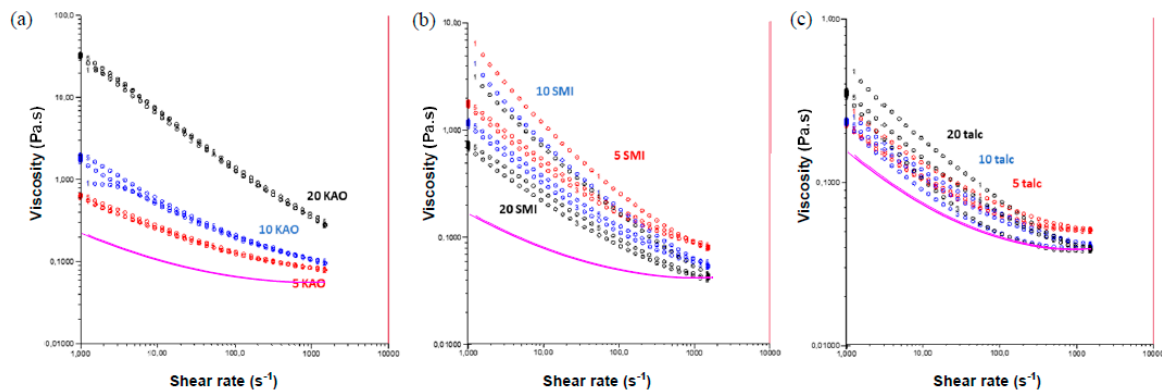

Figure 1. Rheological properties of natural rubber suspensions with different fillers at different concentrations, relative to the unfilled natural rubber suspension (purple curve), (**a**) Kaolinite, (**b**) SMI nanoparticles, (**c**) Talc.

3.2. Microstructural Properties

The effects of fillers on the microstructure of the natural rubber latex are evidenced by results of DSC analysis, as summarized in Figure 2. The pure natural rubber is characterized by a low glass transition temperature of T_g = −64.53 °C and no further thermal transitions were noticed over the temperature range up to 180 °C as no specific vulcanization agents were added. The change in heat capacity Δc_p = 0.4940 J/(g°C) over the glass transition is a measure for the change in the molecular mobility in the amorphous phase during the glass transition and may indicate variations in molecular structure induced—e.g., by chain interactions or cross-linking reactions in the amorphous phase.
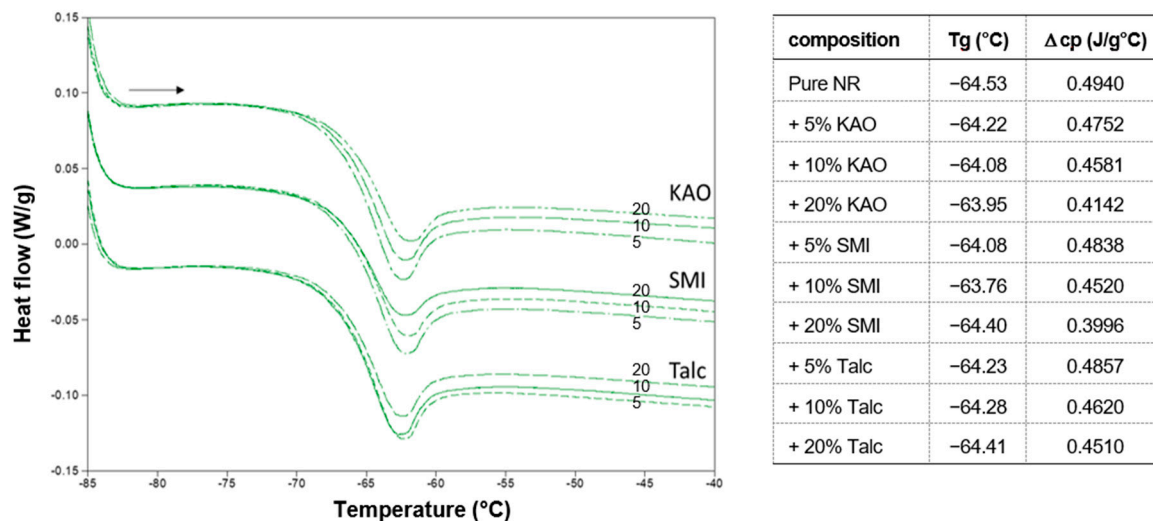

composition	Tg (°C)	Δcp (J/g°C)
Pure NR	−64.53	0.4940
+ 5% KAO	−64.22	0.4752
+ 10% KAO	−64.08	0.4581
+ 20% KAO	−63.95	0.4142
+ 5% SMI	−64.08	0.4838
+ 10% SMI	−63.76	0.4520
+ 20% SMI	−64.40	0.3996
+ 5% Talc	−64.23	0.4857
+ 10% Talc	−64.28	0.4620
+ 20% Talc	−64.41	0.4510

Figure 2. DSC results of natural rubbers with a detail on the glass transition in the presence of different types and concentrations of fillers, listing glass transition temperature T_g and heat capacity change Δc_p (compositions in wt.-%).

The slight but consistent variations in T_g and Δc_p were noticed in the presence of fillers to different extents, depending on the filler type and concentration. A detail of the glass transition step during heating indeed shows either a shift in the temperature T_g and/or a reduction in the value Δc_p in the presence of fillers. The natural rubber composites with fillers show a reduction in Δc_p, relative to the pure natural rubber, which progressively decreases further as a function of higher filler concentrations: the reduction is the highest for the SMI nanoparticles (to a final value of Δc_p = 0.3996

J/(g°C)), the lowest for the talc fillers (to a final value of Δc_p = 0.4510 J/(g°C)), and intermediate for the kaolinite fillers (to a final value of Δc_p = 0.4142 J/(g°C)). This would indicate that the fillers assist in creating cross-links between the molecular chains of the natural rubber, preventing molecular mobility during the glass transition. The nanoparticles are indeed most efficient in creating cross-links, likely due to the surface chemistry of the nanoparticles with residual free amic acid groups and imidized moieties, as detailed before [5], in combination with the nanoscale surface area effect.

The effects of fillers on the structure of natural rubbers are further illustrated from the ATR-FTIR spectra shown in Figure 3. The spectra both confirm the presence of the fillers in different concentrations in parallel with some changes in the natural latex molecular structure. The FTIR spectra of natural rubbers are characterized by the presence of characteristic bands for cis-1,4-polyisoprene, including 2960 cm^{-1} (CH$_3$ symmetric stretching), 2913, 2852 cm^{-1} (CH$_2$ asymmetric and symmetric stretching), 1655 (-C=C-), 1445 cm^{-1} (CH$_3$ and CH$_2$ bending), 1376 cm^{-1} (CH$_3$ bending), and 842 cm^{-1} (=CH wagging). Apart from that, the spectra of different fillers are characterized by separate absorption bands characteristic for SMI nanoparticles: 1713 cm^{-1} (C=O, imide), 701 cm^{-1} (aromatic, styrene); kaolinite: 500 to 700 cm^{-1} (Si-O), 900 cm^{-1} (OH deformation), 1000 cm^{-1} (Si-O stretching) 3600 cm^{-1} (OH stretching, Al-OH stretching); talc: 672 cm^{-1} (Si-O-Si symmetric stretching), 1017 cm^{-1} (Si-O-Si asymmetric stretching), and sharp band at 3670 cm^{-1} (OH).
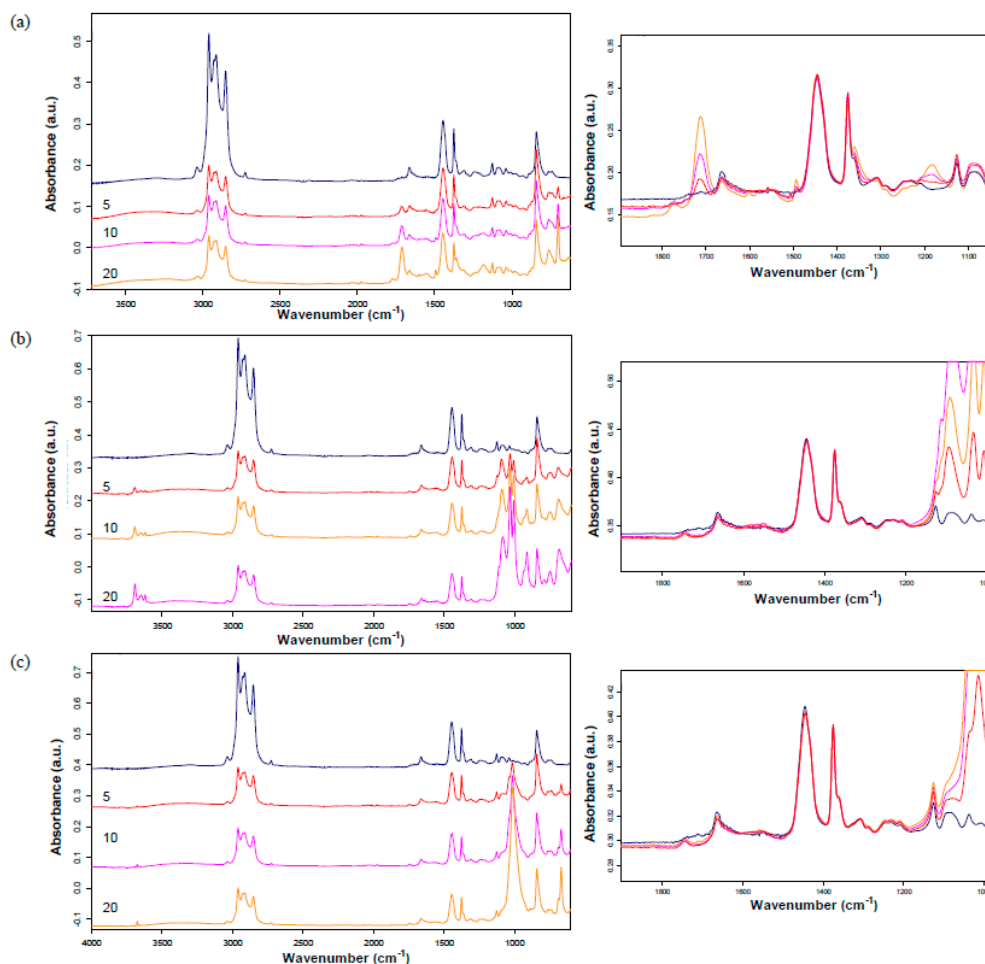

Figure 3. FTIR spectra of natural rubber composites with different concentrations of fillers, (**a**) SMI nanoparticles, (**b**) Kaolinite, (**c**) Talc (same color legends for overview spectra and details on the right).

The related spectral bands of the fillers are independent of the natural rubber matrix and progressively increase at the higher filler concentrations. A single interaction between the SMI nanoparticles and the matrix can be seen at the shoulder peak around 1360 cm^{-1}: the band is present in pure natural rubbers and gradually intensifies with the higher SMI concentrations, while the band

did not appear in single SMI nanoparticles. The latter might indicate physical interactions between the SMI nanoparticles and the CH_3 side groups of the natural rubber polymer chain. In addition, an intensified broad peak over the 3200–3500 cm^{-1} region is most pronounced for the SMI nanoparticle fillers and less present for the kaolinite and talc fillers. This absorption band might be related to the presence of hydroxyl groups that appear to be generated through interactions between the natural rubber with the SMI nanoparticles. On the other hand, no direct changes in the -C=C- double bonds were observed due to chemical cross-linking reactions for either of the fillers. In conclusion, it can be confirmed that strongest physical interactions between the natural rubber matrix and SMI nanoparticles are observed.

3.3. Paper Coating Properties

The morphology of paper surfaces with natural rubber composite coatings are illustrated in Figure 4, representing top views of the different coating compositions. The pure natural rubber coating was fully flat and covered the paper surface as a smooth polymer film. The aspect of kaolinite fillers is observed as a homogeneous and smooth distribution over the coating surface with progressively more dense coverage at the higher concentrations, while they bring good coating density and likely some topographical roughness effects. The SMI nanoparticles are homogeneously distributed within the coating, causing the creation of small micrometer-scale domains. The talc particles are much rougher and are densely present at the surface in an inhomogeneous distribution over the surface. Due to the platelet morphology of talc particles, they are randomly oriented at the surface either perpendicularly sticking out or embedded parallel to the surface.
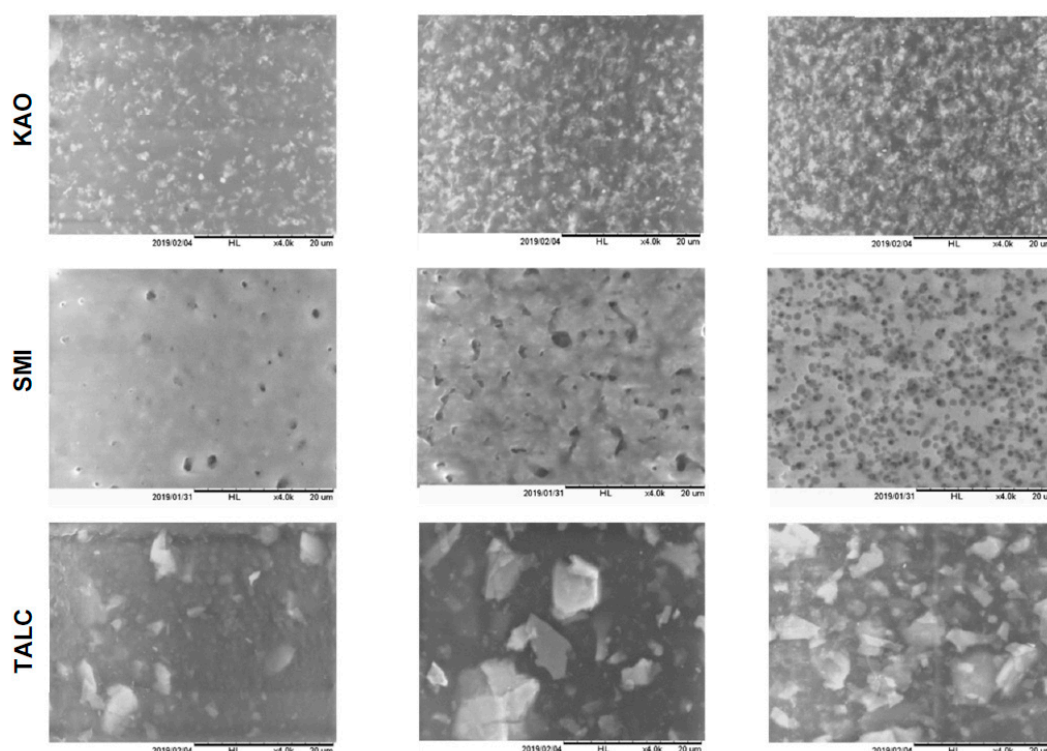

Figure 4. SEM evaluation of natural rubber coatings on paper with different filler types and concentrations (magnification ×4000 for all images).

The results of surface properties, including wetting and adhesive properties, are summarized in bar charts of Figure 5. The static contact angle values of water and diiodomethane in Figure 5a show slight and consistent variations among the different coating types and filler concentrations, relative to the pure natural rubber coating. The contact angles remained stable on the coatings for about 15 seconds, except for the pure natural rubber, as the homogeneity and coverage of the coating was not perfect and fully continuous for the pure natural rubber coating. The exposure of paper fibers at the

surface created voids for the flow of the water through the coating, while the presence of fillers improved the coating coverage and density, providing better bulkiness compared to the pure natural rubber. The original rubber coating had a water contact angle of 95°, being in the hydrophobic range. The presence of kaolinite gradually increases the coating hydrophobicity, likely due to the hydrophobic properties of the fillers in combination with the creation of some additional surface roughness, seen in the microscopic images. The talc particles are hydrophilic, and their properties consequently prevail while exposed at the surface, resulting in a gradual decrease in hydrophobicity with the higher talc concentrations. The hydrophobic properties of SMI nanoparticles are beneficially exploited while added in different concentrations, rising up to a maximum water contact angle of 110°. While the water contact angle indicates the polar interactions, the diiodomethane is an apolar liquid and often shows opposite trends to the water contact angles.
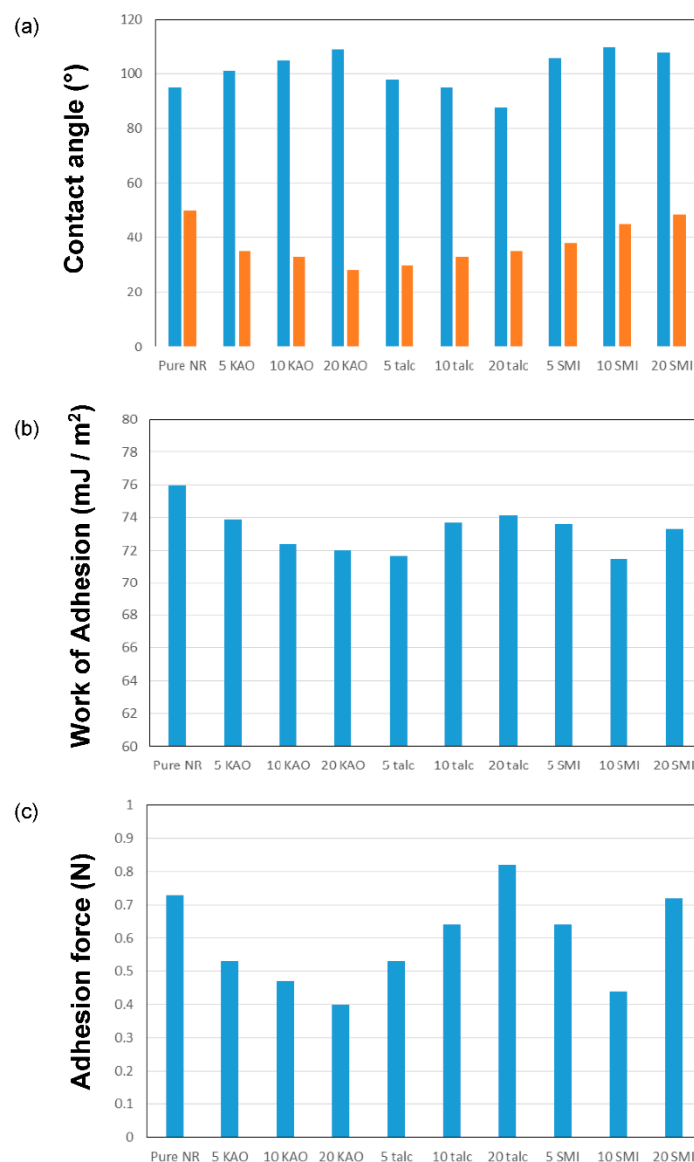

Figure 5. Surface properties of natural rubber coatings on paper substrates, (**a**) static contact angles for water (blue bars) and diiodomethane (orange bars), (**b**) calculated work of adhesion Wa, (**c**) experimental adhesion force from loop test.

The adhesion between coated surfaces of natural rubber composites has been studied in the frame of the tendency for self-adhesion of natural rubber materials. The work of adhesion, Wa = γ_L (1 + cos θ) with γ_L = liquid tension, and taking into account the contact between similar rubber coating materials, can theoretically be calculated from the water and diiodomethane contact angles. The

calculated values are represented in Figure 5b, where it can be noticed that the predicted adhesion varies for the different coating types. The theoretical adhesion is highest for the pure natural rubber and is lower in the presence of filler materials: with increasing filler concentrations, the adhesion gradually decreases in the presence of kaolinite fillers and SMI nanoparticles, while the adhesion increases in the presence of talc particles. This can indeed be related to the hydrophobic effect of the kaolinite and SMI nanoparticles and the hydrophilic effect of the talc particles. The results of experimental adhesion measurements from a loop test with contact between similar rubber composite materials is represented in Figure 5c, and confirm the trends from theoretical calculations. From that, it is mainly revealed that the tendency for adhesion of rubber composite coatings can be predicted from water contact angle measurements and is steered by the hydrophobicity of the coated surface.

4. Conclusions

Different macro- and nanoscale fillers can be homogeneously mixed with a natural rubber latex and applied as a paper coating. The use of hydrophobic nanoparticles shows the most interactions with the latex through interactions with the molecular side chains of the poly-isoprene, while the nanoparticles also provide the highest hydrophobicity and reduced tendency for self-adhesion (tack).

Conflicts of Interest: The authors declare no conflict of interest.

References

1. Panrat, K.; Boonme, P.; Taweepreda, W.; Pichayakorn, W. Formulations of natural rubber latex as film former for pharmaceutical coating. *Proc. Chem.* **2012**, *4*, 322–327.
2. Jianprasert, A.; Monvisade, P.; Yamaguchi, M. Combinatino of tung oil and natural rubber latex in PVA as water based coatings for paperboard application. *MATEC Web Conf.* **2015**, *30*, 03010.
3. Wang, H.; Easteal, A.; Edmonds, N. Prevulcanized natural rubber latex/modified lignin dispersion for water vapour barrier coatings on paperboard packaging. *Adv. Mater. Res.* **2008**, *47–50*, 93–96.
4. Das, D.; Datta, M.; Chavan, R.B.; Datta, S.K. Coating of jute with natural rubber. *J. App. Polym. Sci.* **2005**, *98*, 484–489.
5. Samyn, P.; Deconinck, M.; Schoukens, G.; Stanssens, D.; Vonck, L.; Van den Abbeele, H. Synthesis and characterization of imidized poly(styrene-maleic anhydride) organic nanoparticles in stable aqueous dispersion. *Polym. Adv. Technol.* **2012**, *23*, 311–325.